Investigation of Hybrid Plasma-Catalytic Removal of Acetone over $CuO/\gamma\text{-}Al_2O_3$ Catalysts Using Response Surface Method

Xinbo Zhu[1], Xin Tu[*, 2], Danhua Mei[2], Chenghang Zheng[1], Jinsong Zhou[1], Xiang Gao[*, 1], Zhongyang Luo[1], Mingjiang Ni[1], Kefa Cen[1]

[1] State Key Laboratory of Clean Energy Utilization, Zhejiang University, Hangzhou, 310027, P.R. China

[2] Department of Electrical Engineering and Electronics, University of Liverpool, Liverpool, L69 3GJ, UK

Corresponding Authors

Dr. Xin Tu
Department of Electrical Engineering and Electronics,
University of Liverpool,
Liverpool L69 3GJ
UK
E-mail: xin.tu@liverpool.ac.uk

Prof. Xiang Gao
State Key Laboratory of Clean Energy Utilization,
Zhejiang University,
Hangzhou, 310027,
P.R. China
E-mail: xgao1@zju.edu.cn

Abstract

In this work, plasma-catalytic removal of low concentrations of acetone over CuO/γ-Al_2O_3 catalysts was carried out in a cylindrical dielectric barrier discharge (DBD) reactor. The combination of plasma and the CuO/γ-Al_2O_3 catalysts significantly enhanced the removal efficiency of acetone compared to the plasma process using the pure γ-Al_2O_3 support, with the 5.0 wt.% CuO/γ-Al_2O_3 catalyst exhibiting the best acetone removal efficiency of 67.9%. Catalyst characterization was carried out to understand the effect the catalyst properties had on the activity of the CuO/γ-Al_2O_3 catalysts in the plasma-catalytic reaction. The results indicated that the formation of surface oxygen species on the surface of the catalysts was crucial for the oxidation of acetone in the plasma-catalytic reaction. The effects that various operating parameters (discharge power, flow rate and initial concentration of acetone) and the interactions between these parameters had on the performance of the plasma-catalytic removal of acetone over the 5.0 wt% CuO/γ-Al_2O_3 catalyst were investigated using central composite design (CCD). The significance of the independent variables and their interactions were evaluated by means of the Analysis of Variance (ANOVA). The results showed that the gas flow rate was the most significant factor affecting the removal efficiency of acetone, whilst the initial concentration of acetone played the most important role in determining the energy efficiency of the plasma-catalytic process.

Keywords: Plasma-catalysis; Dielectric barrier discharge; Acetone removal; CuO/γ-Al_2O_3; Response surface method

1. Introduction

Acetone, one of the most abundant oxygenates in air, has been widely used as paint thinner, solvent and raw material in chemical industry. The emission of acetone has negative effects on both the global environment and human health (Koppmann, 2008). Exposure to acetone can cause dizziness, unconsciousness and nausea (Flowers et al., 2003). Great efforts have been devoted to technology research and development to meet the stringent regulations for air pollution control. However, conventional technologies including catalytic combustion, regenerative oxidation, photo-catalytic oxidation, adsorption and condensation are not cost-effective for the removal of low concentrations of acetone in high volume waste gas streams (Schnelle Jr and Brown, 2001).

For the last two decades, non-thermal plasma (NTP) has been regarded as a promising gas cleaning technology for the abatement of low concentration volatile organic compounds (VOCs) in high volume waste gas streams (Chen et al., 2009; Tu and Whitehead, 2012). Using air as a carrier gas, energetic electrons and a large number of highly reactive species including O, O_3, N and metastable N_2 can be generated in the plasma even at room temperature. Both high energy electrons and reactive species are capable of initiating a cascade of physical and chemical reactions, which contribute to the removal of gas pollutants. The main challenges in the industrial application of NTP for waste gas clean-up are the formation of unwanted by-products and the low energy efficiency of the plasma process (Kogelschatz, 2003; Kim, 2004). CO, CH_4, HCOOH and HCHO were found to be the major organic by-products in plasma decomposition of acetone (Lyulyukin et al., 2010; Narengerile and Watanabe, 2012; Zheng et al., 2014).

Recently, the combination of plasma and heterogeneous catalysis, namely plasma-catalysis, has been considered as a promising solution for waste gas clean-up. The presence of a catalyst in the plasma has great potential to generate a synergistic effect, which

can reduce the activation energy of the reaction, enhance the removal of the gas pollutant and the selectivity of the desired final products, and minimize the formation of unwanted by-products. All of these contribute in different ways to increasing the energy efficiency of the plasma-catalytic process (Van Durme et al., 2008; Chen et al., 2009; Vandenbroucke et al., 2011). Chang and Lin (2005) reported the acetone decomposition efficiency of a plasma process to be 25% higher in the presence of TiO_2 compared to that using NTP alone. Trinh and Mok (2014) found that placing ceramic supported MnO_2 catalysts in a dielectric barrier discharge (DBD) significantly improved the removal efficiency of acetone, by 37%, at a specific energy density (SED) of 600 J L^{-1}. In our previous work, we showed that the energy yield of acetone removal (3.72 g kWh^{-1}) was 51.0% higher in the presence of γ-Al_2O_3 than when using plasma alone (Zheng et al., 2014).

Catalysts are of great significance in a plasma-catalysis system. Various catalysts have been reported for plasma-catalytic oxidation of VOCs, among which Cu-based catalysts showed their advantages over other transition metal oxide catalysts due to their low cost and comparative reaction performance (Guo et al., 2007; An et al., 2011; Wu et al., 2013; Zhu et al., 2015a). Our previous work showed that the addition of 10 wt% transition metal oxides (Ce, Co, Cu, Mn and Ni) on γ-Al_2O_3 support enhanced the removal of acetone, with the supported copper oxide catalyst exhibiting the best performance among the tested transition metals (Zhu et al., 2015b).

Although plasma-catalytic removal of acetone has been reported before, far less has been done for the optimization of the plasma-catalytic process since its reaction performance is largely affected by various operation parameters (Vandenbroucke et al., 2011; Samukawa et al., 2012). The optimization of plasma-catalytic systems in previous work has been mostly carried out via experimental approaches. The traditional univariate method fails to consider and represent the interactions between different input variables. Moreover, this method

requires a large amount of experimental data to obtain the favorable sets of operating parameters for the optimization of the plasma process, which makes it time consuming and labor intensive (Aerts et al., 2013; Thevenet et al., 2014; Xu et al., 2014). Recently, response surface methodology (RSM) has drawn attention for the investigation and optimization of processes. RSM is a statistical model considering the non-linear relationships between the multiple input and output variables based on design of experiments (DoE), which aims to predict and optimize the performance of complex systems via experiment design, model building, and evaluation of the significance of independent variables and the interactions between them. Until now, only limited work has been focused on the investigation of plasma processes using the DoE method (Butron-Garcia et al., 2015; Mei et al., 2015), while the use of DoE for the optimization of plasma-catalytic gas clean-up has not been reported before.

In this work, the effect of discharge power, gas flow rate, initial acetone concentration and Cu loading amount on the performance of the plasma-catalytic removal of acetone were investigated. Initial experiments were carried out to find an optimal Cu loading amount for the highest removal efficiency of acetone. A series of catalyst characterization techniques were performed to establish the relationships between catalyst properties and reaction performance. A central composite design (CCD) method was applied to investigate the interactions between the main process variables and to optimize the plasma-catalytic process in terms of removal efficiency and energy efficiency.

2. Experimental

2.1 Catalyst preparation and characterization

The x wt% $CuO/\gamma\text{-}Al_2O_3$ catalysts (x=2.5, 5.0, 7.5 and 10.0) were prepared by incipient wetness impregnation using copper nitrate (Alfa Aesar, 99.5%) as the precursor. The appropriate weight of support ($\gamma\text{-}Al_2O_3$) was added to the copper nitrate solution with a

concentration of 0.1 M and continuously stirred at 80 °C for 4 h. The resulting slurry was dried in an oven at 110 °C overnight, followed by calcination at 500 °C for 5 h. Pure γ-Al_2O_3 support was treated in the same way for comparison in this study. All the catalysts were sieved to 40-60 meshes prior to use.

The structural properties of the CuO/γ-Al_2O_3 catalysts, including specific surface area, average pore size and pore volume, were acquired via N_2 adsorption-desorption experiments using a Quantachrome Autosorb-1 instrument at -196 °C. The X-ray diffraction (XRD) patterns of the catalyst samples were analyzed by a Rikagu D/max-2000 X-ray diffractometer. The instrument was equipped with a Cu-Kα radiation source, with the scan conducted in the 2θ range from 10 ° to 80 ° with a scanning rate of 4 ° min^{-1} and a step size of 0.02°. The reducibility of the CuO/γ-Al_2O_3 catalysts was evaluated by temperature-programmed reduction with hydrogen (H_2-TPR) using a gas chromatograph (GC-1690). Each catalyst (50 mg) was pre-treated at 200 °C in a N_2 flow for 1 h before the test. The samples were then heated from room temperature to 800 °C at a heating rate of 10 °C·min^{-1}. A 5% H_2/Ar flow with a flow rate of 40 mL min^{-1} was used. The amount of consumed H_2 was calculated by the integration of the H_2-TPR signals.

2.2 Experimental set-up

The schematic diagram of the experimental set-up is shown in Fig. 1. A 60 mm-long aluminum foil (ground electrode) was wrapped over a quartz tube with an inner diameter of 8 mm and wall thickness of 1 mm. A stainless steel rod with an outer diameter of 4 mm was placed in the axis of the quartz tube and acted as a high voltage electrode. The length of the discharge zone was 60 mm with a discharge gap of 2 mm. Zero grade air (99.999%) was used as carrier gas in this work. Gaseous acetone was generated from a gas cylinder (0.5% acetone, balanced air). All gas streams were controlled by mass flow controllers and premixed prior to

the DBD reactor. In each experiment, catalyst samples with a dielectric constant of around 12.6 were placed in the discharge region, held in place by glass wool. The reactor was powered by an AC power supply with a frequency of 10.2 kHz, while the maximum peak voltage was 30 kV.

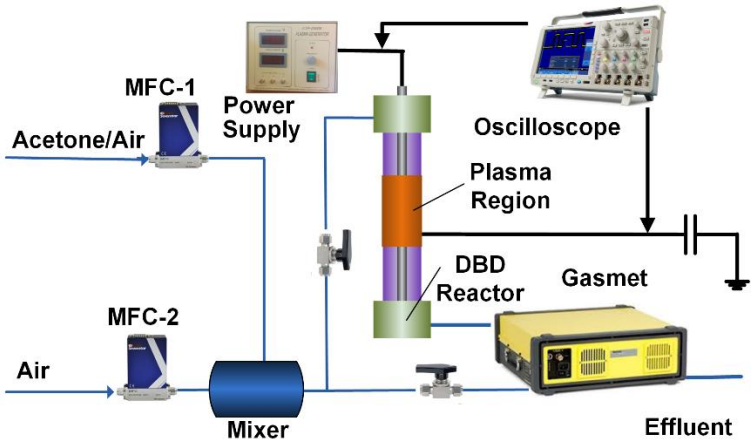

Fig. 1. Schematic diagram of the experimental setup

The applied voltage was measured by a Tektronix 6015A high voltage probe (1000:1), while the voltage across the external capacitor (0.47 μF) was monitored by a Tektronix TPP500 probe. All electrical signals were sampled by a digital oscilloscope (Tektronix 3034B). The discharge power was calculated using Q-U Lissajous method.

Gas products were measured by an online multi-component analyzer (Gasmet Dx4000, Finland) with a resolution of 8 cm^{-1}. The Gasmet was calibrated with a standard acetone gas cylinder (1%, air balanced). The effective path length of the gas analyzer was 5 m, while the volume of the gas cell was 0.4 L. Measurements were carried out after running the plasma reaction for about 40 min, when a steady-state of the process was reached. All experimental data were obtained by repeating 3 times, with the average value of the three measurements being presented. The removal efficiency of acetone ($\eta_{acetone}$) and energy efficiency (*EE*) of the plasma-catalytic process can be defined as:

$$\eta_{\text{acetone}} = \frac{c_{in} - c_{out}}{c_{in}} \times 100\% \quad (1)$$

$$EE\,(g\ kWh^{-1}) = \frac{M_{acetone} \times \eta_{acetone} \times c_{\text{in}} \times Q}{P \times V_m} \times 3.6 \times 10^6 \quad (2)$$

where c_{in} and c_{out} are the inlet and outlet acetone concentration (ppm); $M_{acetone}$ is the molar weight of acetone ($g\,mol^{-1}$); Q is the total flow rate ($L\,min^{-1}$), P is the discharge power (W) and V_m is the gas molar volume.

2.3 Response surface exploration

In this work, a three-factor, five-level central composite design was used to investigate the effects of the independent variables and the interactions of these factors on plasma-catalytic removal of acetone using the trial version of Design-Expert® 8.05b (Stat-Ease Inc., Minneapolis, USA). Three plasma process parameters, discharge power (X_1), gas flow rate (X_2), and the initial concentration of acetone (X_3), were chosen as the input factors for the design, while the removal efficiency (Y_1) and energy efficiency (Y_2) of the plasma-catalytic process were employed as the responses based on our previous work [19]. A total of 20 experiments including 6 axial points, 8 factorial points and 6 replicates at the central point were designed using the CCD method (Table 1). Each input parameter was coded into five levels as –2, -1, 0, +1 and +2 according to Eq. (3):

$$x_i = \left(X_i - X_0\right) / \Delta X_i \quad (3)$$

where x_i is the coded value of the i^{th} variable, X_i is the original value of the i^{th} variable, X_0 is the value of X_i at the centre point of the tested data range and ΔX_i is the step size. The levels

of the selected plasma processing parameters were given in both coded and real values (**Table 1**).

Table 1. Independent variables and their levels used in the CCD method.

Symbols	Variables	Ranges and levels				
		-2	–1	0	+1	+2
x_1	Discharge power (W)	15	17.5	20	22.5	25
x_2	Gas flow rate ($L \cdot min^{-1}$)	0.5	0.75	1	1.25	1.5
x_3	Initial concentration of acetone (ppm)	100	150	200	250	300

In the CCD design, a quadratic polynomial response equation was used to correlate and describe the relationship between the independent plasma processing parameters and the responses:

$$Y = \beta_0 + \sum_{i=1}^{k} \beta_i x_i + \sum_{i=1}^{k} \beta_{ii} x_i^2 + \sum \sum_{i<j} \beta_{ij} x_i x_j + \varepsilon \quad (4)$$

where Y, k, x_i and ε are the response, the number of variables, the coded values of independent variables and the residual value, respectively. β_0 is a constant coefficient, whilst β_i. β_{ii} and β_{ij} are linear, quadratic and interaction coefficients, respectively. The quality of fit and the significance of the polynomial model can be identified by the coefficient of determination (R^2) and the *F*-test, which were completely analyzed by the analysis of variance (ANOVA). The interactions of the independent variables were investigated by constructing the response surfaces and contour plots based on the model (Montgomery et al., 1984).

3. Results and discussions

3.1 Catalysts characterizations

The physicochemical properties of the $CuO/\gamma\text{-}Al_2O_3$ catalysts were analyzed by N_2 adsorption-desorption experiments. The isotherms of all the catalysts are of typical type V, while the hysteresis loops exhibit type H4, indicating the formation of narrow slit-like pores in the catalysts (Lippens and De Boer, 1965; Sing, 1985). The $\gamma\text{-}Al_2O_3$ support has a large specific surface area (241.6 $m^2 g^{-1}$) and a well-developed total pore volume (0.377 $cm^3 g^{-1}$). The specific surface area and total pore volume of the $CuO/\gamma\text{-}Al_2O_3$ catalysts decreases from 209.6 to 187.8 $m^2 g^{-1}$ and from 0.338 to 0.299 $cm^3 g^{-1}$ in the Cu loading amount range of 2.5% to 10%, which can be attributed to the partial coverage of the $\gamma\text{-}Al_2O_3$ surface by Cu species. In contrast, the average pore diameter slightly increases from 5.01 to 5.19 nm, indicating the clogging of micro-pores in the presence of Cu species (Zakaria et al., 2012).

Table 2. Physicochemical properties of $CuO/\gamma\text{-}Al_2O_3$ catalysts.

Sample	S_{BET} ($m^2 g^{-1}$)	Total pore volume ($cm^3 g^{-1}$)	Average pore diameter (nm)	Amount of H_2 consumed ($\mu mol\ g^{-1}$)
$\gamma\text{-}Al_2O_3$	241.6	0.377	4.99	-
2.5 wt % $CuO/\gamma\text{-}Al_2O_3$	209.6	0.338	5.01	233.4
5.0 wt % $CuO/\gamma\text{-}Al_2O_3$	206.7	0.324	5.07	422.7
7.5 wt % $CuO/\gamma\text{-}Al_2O_3$	192.8	0.315	5.14	594.0
10.0 wt % $CuO/\gamma\text{-}Al_2O_3$	187.8	0.299	5.19	791.9

The XRD patterns of the $CuO/\gamma\text{-}Al_2O_3$ catalysts and $\gamma\text{-}Al_2O_3$ support are shown in Fig. 2. All the catalysts show diffraction peaks that correspond to the typical cubic structure of $\gamma\text{-}Al_2O_3$ crystalline (JCPDS 00-010-0425). No obvious diffraction peaks ascribed to the crystalline phase of copper oxides are observed at low Cu loading (2.5 wt % and 5.0 wt%), which suggests the Cu species are well dispersed on the $\gamma\text{-}Al_2O_3$. The diffraction peaks of

crystalline CuO (JCPDS 01-089-5899) located at 2θ=35.5° and 38.8° are clearly seen when increasing the Cu loading amount, indicating the formation of bulk CuO at high Cu loading (7.5 wt % and 10.0 wt%).

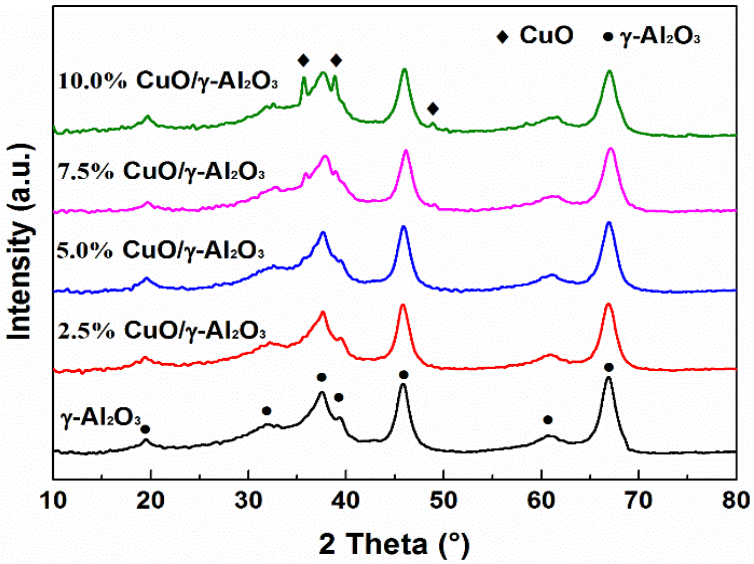

Fig. 2. XRD patterns of the CuO/γ-Al_2O_3 catalysts.

Fig. 3 shows the H_2-TPR profiles of all the CuO/γ-Al_2O_3 catalysts used in this study as the γ-Al_2O_3 support cannot be reduced within the tested temperature range (Zhu et al., 2015b). The amounts of consumed H_2 were calculated based on the H_2-TPR profiles. As expected, the intensities of the reduction peaks increase significantly with increasing Cu loading amount. It can be seen that there exists a single reduction peak located at around 240 °C at the Cu loading amount of 2.5 wt%. At higher Cu loading amounts, the reduction peaks are shifted to lower temperatures. At low loading amount, the existence of isolated Cu species was dominant, leading to a higher reduction temperature (Yamamoto et al., 2002). For the other catalysts, the H_2-TPR profiles show two distinct peaks. The first peak can be attributed to the reduction of highly dispersed CuO species, while the second peak is associated with the reduction of bulk CuO (Águila et al., 2008). The XRD spectra also confirm the existence of bulk CuO at the Cu loading amounts of 7.5 wt% and 10 wt%. The lowest reduction

temperature of 182 °C can be observed for the 5.0 wt% CuO/γ-Al_2O_3 catalyst, indicating that it is easy to activate oxygen species on the surface of the 5.0 wt% CuO/γ-Al_2O_3 catalyst. At the Cu loading amounts of 7.5 wt% and 10 wt%, the reduction peaks shift to higher temperatures (López-Suárez et al., 2008).

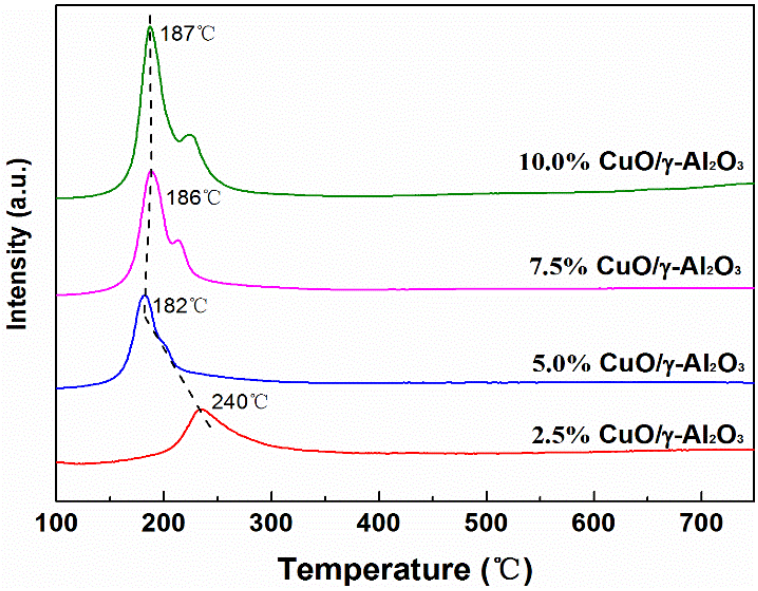

Fig. 3. H_2-TPR profiles of CuO/γ-Al_2O_3 catalysts.

3.2 Plasma-catalytic removal of acetone

Fig. 4 shows the effect of Cu loading on the plasma-catalytic removal of acetone. The removal of acetone increases monotonically with increasing discharge power regardless of the Cu loading amount. The maximum acetone removal efficiency of 67.9% was achieved at a discharge power of 25 W in the presence of the 5.0 wt% CuO/γ-Al_2O_3. It is widely recognized that higher discharge power could lead to the formation of more microdischarges in the DBD, which generates more reaction channels and chemical reactive species (e.g., O, O_3, N and metastable N_2) for chemical reactions. These reactive species collide and react with acetone and intermediates, forming reaction products including organic fragments, CO, CO_2 and H_2O. Hence, higher discharge power improves the removal efficiency of acetone in the plasma-catalytic process.

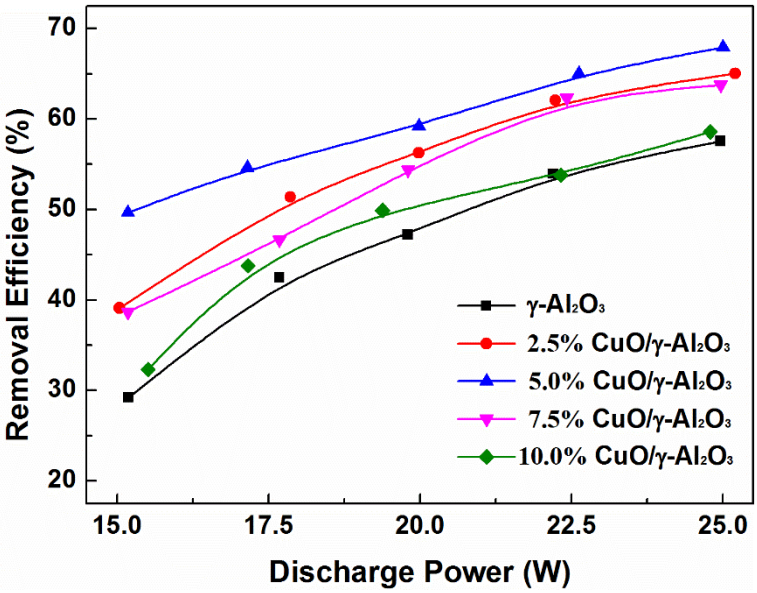

Fig. 4. Effect of Cu loadings on the plasma-catalytic removal of acetone.

The Cu loading amount significantly affects the reaction performance of the plasma-catalytic oxidation of acetone in the tested discharge power range. The acetone removal efficiency increases with the Cu loading amount up to 5%, while further increasing the Cu loading decreases the reaction performance of the plasma-catalytic process. The catalysts play an important role in the plasma-catalytic system for VOC removal. In the presence of the catalysts, acetone molecules and the organic fragments could be adsorbed and oxidized to CO_2 and H_2O via surface reactions on the surface of the catalysts (Zhu et al., 2015a). The different reaction performances might be attributed to the different physicochemical properties of the CuO/γ-Al_2O_3 catalysts.

As presented in section 3.1, all the CuO/γ-Al_2O_3 catalysts possessed comparable specific surface area, with no obvious changes found in the structure and crystallites of the catalysts. The large specific surface area of the catalysts could offer many adsorption sites for acetone molecules and intermediates, resulting in a longer residence time of the pollutants in the plasma region and benefitting the removal of acetone. The adsorbed species are further converted via surface reactions driven by surface oxygen species. The H_2-TPR profiles show

that the most easily reducible Cu species (corresponding to the first peak in H_2-TPR profiles) increase significantly from 2.5 wt% CuO/γ-Al_2O_3 to 5.0 wt% CuO/γ-Al_2O_3, and continue to slightly increase for higher Cu loadings, indicating the abundance of surface oxygen species with high mobility which could participate in the plasma-induced surface reactions. López-Suárez et al. (2008) reported that a maximum surface Cu loading amount on Al_2O_3 can be achieved at around 5.0 wt% Cu loading, with further addition of Cu decreasing the surface Cu amount. This is in line with the formation of bulk CuO at a high Cu loading amount derived from the XRD results, which could in turn inhibit the surface reactions (Luo et al., 2005). Among the tested catalysts the lowest reduction temperature is found when using the 5.0 wt% CuO/γ-Al_2O_3 catalyst, indicating easier activation of the catalyst. This is closely related to the redox properties of the catalyst and consequently affects the reaction performance.

The main gaseous products in the effluent were CO, CO_2 and H_2O, while small amounts of HCOOH, HCHO, NO_2 and N_2O were also detected. The removal of acetone in the plasma-catalytic process could be attributed to the combination of plasma-induced gas phase reactions and plasma-assisted surface reactions on the CuO/γ-Al_2O_3 catalysts. The plasma gas phase reactions for acetone removal were initiated by direct electron impact dissociation of the carrier gas (air) to form chemically reactive species such as O, OH, N and metastable N_2 for the stepwise decomposition and oxidation of acetone and/or intermediates into CO, CO_2, H_2O and other by-products (Fridman, 2008). Acetone molecules can be decomposed by the rupture of C-C and C-H bonds, forming methyl groups (CH_3·) and acetone groups (CH_3COCH_2·). Consequently, acetone radicals can be oxidized by O and OH to acetyl radicals, methyl groups and ketenes. The further oxidation of acetyl radicals leads to the formation of methanol and acetic acid (Magne et al., 2009). Methyl groups can be further decomposed to CH and CH_2 by energetic electrons (Huang et al., 2011). These species can

311 react with O and OH radicals, forming CO, CO_2, HCHO and HCOOH. In the plasma-catalytic
312 process, catalysts were placed in the plasma region in direct contact with the discharge. Both
313 short-lived radicals and acetone/intermediates can be adsorbed on the catalyst surfaces to
314 initiate a series of surface oxidation reactions, forming CO, CO_2, H_2O and by-products.
315
316 **3.3 DoE analysis**
317 **3.3.1 Regression models and data analysis**
318 In this work, optimization of the plasma-catalytic removal of acetone was carried out
319 using the CCD method in the presence of the most active catalyst (5.0 wt% CuO/γ-Al_2O_3).
320 The designed experiments and corresponding results of the CCD method are summarized in
321 **Table 3**. The removal efficiency of plasma-catalytic removal of acetone varies from 44.3% to
322 81.3%, while the energy efficiency of the plasma-catalytic process is in the range of 0.60 g
323 kWh^{-1} to 1.30 g kWh^{-1}. The obtained responses were correlated to the aforementioned
324 independent plasma processing parameters using the polynomial equation (4). The best-fit
325 models of removal efficiency and energy efficiency in terms of coded factors are as follows:

$$Removal\ Efficiency(\%):$$

326
$$Y_1 = 59.69 + 4.75x_1 - 8.43x_2 - 4.99x_3 + 0.74x_1x_2 - 0.67x_1x_3 + 1.86x_2x_3 + 0.075x_1^2 + 0.72x_2^2 + 0.79x_3^2 \quad (5)$$

$$Energy\ Efficiency\left(g \cdot kWh^{-1}\right):$$

327
$$Y_2 = 0.92 - 0.043x_1 + 0.11x_2 + 0.16x_3 + 0.012x_1x_2 - 0.015x_1x_3 + 0.04x_2x_3 + 7.222\times10^{-3}x_1^2 - 0.021x_2^2 - 7.736\times10^{-3}x_3^2 \quad (6)$$

328
329 **Table 3.** Experimental design matrix and experimental results of the CCD

Run order	Coded values (X)			Responses (Y)	
	Discharge power (x_1)	Gas flow rate (x_2)	Initial concentration (x_3)	Y_1: Removal efficiency (%)	Y_2: Energy efficiency (g kWh^{-1})

1	20	1	200	59.3	0.91
2	20	1	200	59.2	0.91
3	20	0.5	200	78.5	0.60
4	15	1	200	49.7	1.02
5	20	1	200	59.5	0.92
6	17.5	0.75	250	59.7	0.98
7	20	1	300	51.1	1.18
8	22.5	0.75	250	68.7	0.88
9	22.5	1.25	250	55.4	1.18
10	20	1	200	59.3	0.91
11	17.5	1.25	250	47.2	1.30
12	25	1	200	67.9	0.84
13	22.5	0.75	150	81.3	0.63
14	20	1.5	200	44.3	1.02
15	20	1	100	72.2	0.56
16	22.5	1.25	150	64.3	0.82
17	20	1	200	59.2	0.91
18	17.5	0.75	150	73.4	0.73
19	20	1	200	59.3	0.91
20	17.5	1.25	150	49.7	0.82

Table 4 shows the ANOVA of the generated regression models. The results confirm that the models are highly significant since the F-values for both Y_1 and Y_2 are found to be 72.33 and 83.20, both of which are greater than the critical value of 3.02 in our case (Montgomery et al., 1984). Moreover, the ultimate low probability value (p-value < 0.0001) indicates the significance of both models at a confidence level greater than 95%. It can be confirmed that most variations in the response can be explained by the generated models considering the high

F-values and low *p*-values. The obtained regression correction coefficients (R^2) (0.9849 for Y_1 and 0.9868 for Y_2) are close to unity, indicating the regression models are well fitted to the experimental results. The adequate precision presents the signal-to-noise ratio of the models, while values greater than 4 are desirable. In this study, the adequate precisions are 29.645 and 32.610 for the removal efficiency and energy efficiency of the plasma-catalytic process, respectively, which indicate adequate intensities of the signals. The coefficients of variations (C.V.), as the ratio of the standard error of the estimations to the mean value of the responses, could be used to measure the reproducibility of the regression models. The obtained C.V. are 2.84% for Y_1 and 3.33% for Y_2, which are less than the critical value of 10%, indicating the reliability and reproducibility of the models (Mousavi et al., 2014).

Table 4. ANOVA of magnitude and significance of factor effects on the responses

Response	Model terms	Sum of square	Degree of freedom	Mean square	*F*-value	*p*-value (Prob.>*F*)
Removal Efficiency	Model	1957.54	9	217.50	72.33	< 0.0001
	x_1	361.50	1	361.50	120.22	< 0.0001
	x_2	1137.46	1	1137.46	378.28	< 0.0001
	x_3	398.40	1	398.40	132.49	< 0.0001
	x_1x_2	4.43	1	4.43	1.47	0.2527
	x_1x_3	3.58	1	3.58	1.19	0.3005
	x_2x_3	27.58	1	27.58	9.17	0.0127
	x_1^2	0.14	1	0.14	0.047	0.8333
	x_2^2	13.01	1	13.01	4.33	0.0642
	x_3^2	15.62	1	15.62	5.19	0.0459
	Residual	30.07	10	3.01		
	Total	1987.61	19			

		R^2=0.9849, Adequate precision=29.645, C.V.=2.84%				
Energy Efficiency	Model	0.67	9	0.075	83.20	< 0.0001
	x_1	0.029	1	0.029	32.14	0.0002
	x_2	0.19	1	0.19	211.41	< 0.0001
	x_3	0.42	1	0.42	469.64	< 0.0001
	x_1x_2	1.152E-3	1	1.152E-3	1.28	0.2843
	x_1x_3	1.872E-3	1	1.872E-3	2.08	0.1797
	x_2x_3	0.013	1	0.013	14.46	0.0035
	x_1^2	1.311E-3	1	1.311E-3	1.46	0.2551
	x_2^2	0.012	1	0.012	12.88	0.0049
	x_3^2	1.505E-3	1	1.505E-3	1.67	0.2250
	Residual	8.997E-3	10	8.997E-4		
	Total	0.68	19			
		R^2=0.9868, Adequate precision=32.610, C.V.=3.33%				

3.3.2 Effect of variables on removal efficiency

A model term is considered to play an important role in the plasma-catalytic process once its p-value is below the level of significance (0.05 in this work). In the plasma-catalytic removal of low concentrations of acetone, x_1, x_2, x_3, x_2x_3 and x_3^2 are identified as the significant terms for the removal efficiency of acetone, while x_1, x_2, x_3, x_2x_3 and x_2^2 are important for the energy efficiency of the plasma-catalytic process. Considering the highest F-value of 378.22, the air flow rate is believed to be the most important factor affecting the removal efficiency of the plasma-catalytic process. Similarly, the largest *F*-value of initial concentration confirms its role in determining the energy efficiency of the process.

Three-dimensional (3D) response surfaces and two-dimensional (2D) contours are presented (**Fig. 5 - Fig. 7**) based on the quadratic polynomial regression models to gain new

insights into the effects of each individual factor and their interactions on the plasma-catalytic process. **Fig. 5** shows the combined effect of discharge power and flow rate on the removal and energy efficiency at the initial acetone concentration of 200 ppm (the center level). The acetone removal efficiency increases significantly with an increase in the discharge power and flow rate (shown in **Fig. 5**a). The maximum acetone removal efficiency of 86.2% is achieved at a discharge power of 25 W and a flow rate of 0.5 L min^{-1}. As discussed earlier, the number of micro-discharges increases with increasing discharge power, which could contribute to the generation of more reaction channels and reactive species, and consequently enhance the reaction performance. Significant decreases in removal efficiency are observed with increasing flow rate. The residence time of pollutants at 0.5 L min^{-1} is 3 times that at 1.5 L min^{-1}. Longer residence time is beneficial for the removal of acetone as the possibility of collisions between the reactive species and the pollutants is much higher than at shorter residence times. The highest energy efficiency of 1.12 g kWh^{-1} is obtained at a discharge power of 15 W and flow rate of 1.5 L min^{-1}, which may be attributed to heating and excitation of the carrier gas by the dissipated discharge power. Similar observations have been reported elsewhere in cases of VOC removal using either DBD reactors or packed-bed reactors (Zheng et al., 2014). The interactions between the two terms on the reaction performance are regarded as insignificant as the gradients are almost the same at varied flow rates and discharge powers, while the contours are almost linear (Mei et al., 2015). The *p*-values of 0.2527 and 0.2843 (greater than the critical value of 0.05) also support this conclusion.

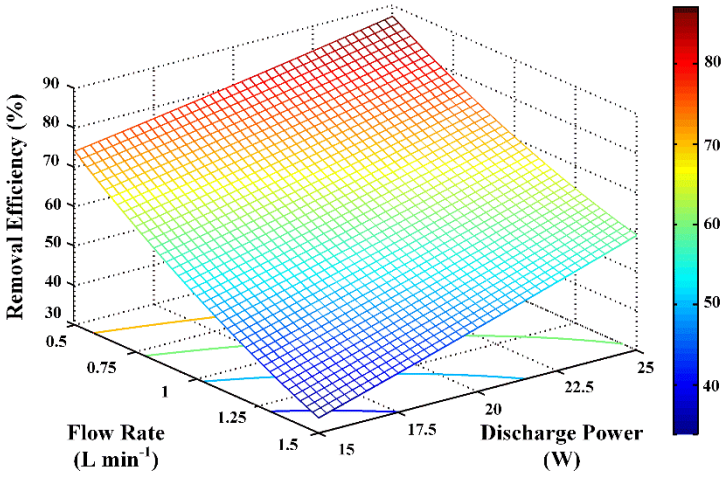

(a)

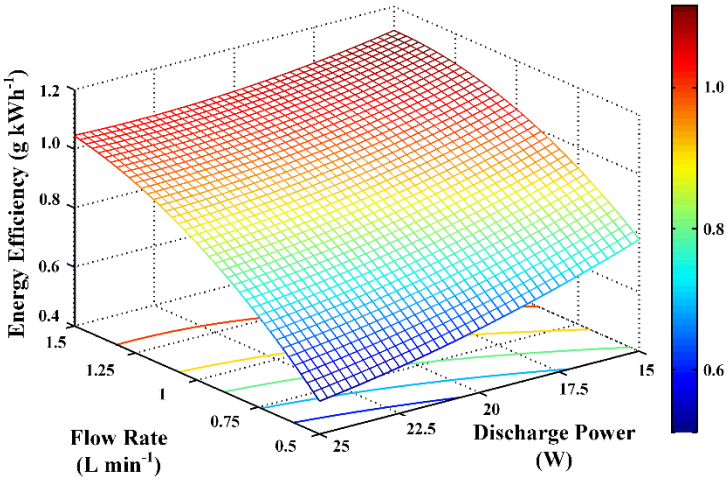

(b)

Fig. 5. Effect of discharge power and flow rate on plasma-catalytic removal of acetone at the initial concentration of 200 ppm: (a) removal efficiency; (b) energy efficiency.

Fig. 6 illustrates the effect of discharge power and initial concentration on plasma-catalytic removal of acetone. The maximum acetone removal efficiency of 85.2% is obtained at a discharge power of 25 W and an initial acetone concentration of 100 ppm, while the highest energy efficiency of 1.51 g kWh^{-1} is reached at an initial concentration of 300 ppm and a discharge power of 15 W. The removal efficiency of acetone is doubled when the

discharge power is increased from 15 W to 25 W at 100 ppm, but only increases by 34.8% at an initial concentration of 300 ppm. Higher initial concentration of acetone exhibits a negative effect on acetone removal regardless of the discharge power. For constant reactor and operation parameters, the generation of reactive radicals in the plasma process is almost the same (Nie et al., 2013). At higher initial concentration, more acetone molecules are introduced into the plasma-catalytic system, whilst the concentration of reactive species has been diluted, which lowers the probability of acetone molecules reacting with these reactive species. Consequently, the removal efficiency of acetone decreases with increasing initial concentration. On the other hand, higher initial concentration enhanced the chance of reactions occurring between reactive species and methanol molecules, which led to better utilization of the reactive species. At this point, more acetone molecules can be converted and the energy efficiency of the plasma process is increased at higher initial concentration. The interaction between the discharge power and initial concentration is not significant as the contour lines are linear and the *p*-values are greater than 0.05, namely 0.3005 for removal efficiency and 0.1797 for energy efficiency.

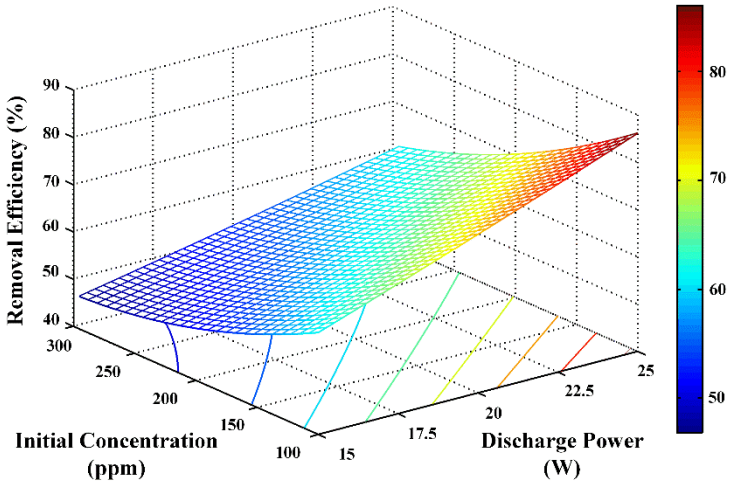

(a)

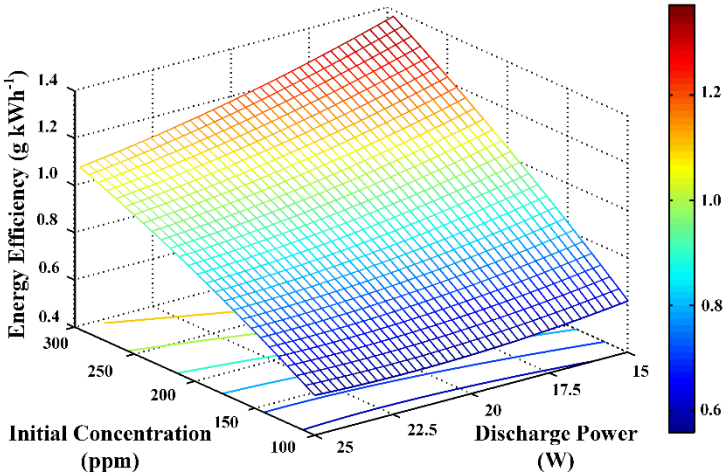

(b)

Fig. 6. Effect of discharge power and initial concentration on plasma-catalytic removal of acetone at the flow rate of 1 L min^{-1}: (a) removal efficiency; (b) energy efficiency.

The effect of flow rate and initial concentration on the performance of plasma-catalytic removal of acetone is plotted in **Fig. 7**. The two terms exhibit a similar effect on the process performance as discussed before. The highest removal efficiency of 99.8% is obtained at a gas flow rate of 0.5 L min^{-1} and an initial concentration of 100 ppm, while the maximum energy efficiency is reached at a flow rate of 1.5 L min^{-1} and an initial concentration of 300 ppm. The removal efficiency of acetone appears to be more sensitive to the flow rate as the gradient of the removal efficiency is much larger at 100 ppm compared to that at 300 ppm, while the initial concentration of acetone is more important for improving the energy efficiency, considering the energy efficiency of the plasma process is almost independent at 100 ppm. This can also be confirmed by the *F*-values of each term for Y_1 and Y_2 in **Table 4**. Moreover, the low *p*-value (<0.001) of the term x_2x_3 also confirms the strong interactions between initial concentration and flow rate and the effect these have on the reaction performance of plasma-catalytic removal of acetone.

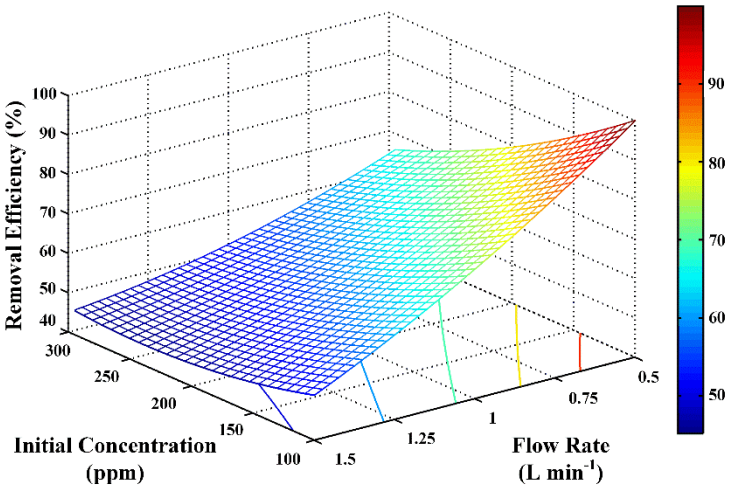

(a)

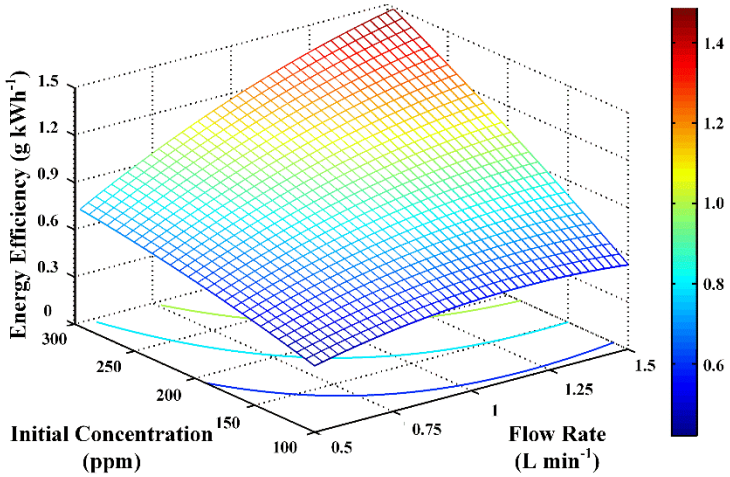

(b)

Fig. 7. Effect of flow rate and initial concentration on plasma-catalytic removal of acetone at a discharge power of 15 W: (a) removal efficiency; (b) energy efficiency.

4. Conclusions

In this work, the plasma-catalytic removal of acetone was investigated using a series of CuO/γ-Al_2O_3 catalysts. The integration of plasma with the CuO/γ-Al_2O_3 catalysts significantly improves the removal efficiency of the plasma-catalytic gas cleaning process by 15% to 20% in the tested discharge power range compared to the plasma process using pure γ-Al_2O_3

support. The 5.0 wt% $CuO/\gamma\text{-}Al_2O_3$ catalyst exhibits the best activity with the maximum acetone removal efficiency of 67.9% at a discharge power of 25 W. Catalyst characterization including BET, XRD and H_2-TPR demonstrates that the activation of surface oxygen species were crucial for the oxidation of acetone molecules and organic by-products on the catalyst surface, which in turn enhances the reaction performance.

The effects of various plasma operating parameters, including discharge power, flow rate and initial concentration of acetone, on the plasma-catalytic process and the interactions between these parameters were investigated using CCD method in the presence of the 5.0 wt% $CuO/\gamma\text{-}Al_2O_3$ catalyst. The generated regression models fits very well with the actual data considering the high coefficient of determination (R^2=0.9849 for removal efficiency and 0.9868 for energy efficiency). The ANOVA results show that the flow rate was the most significant factor affecting the removal efficiency of acetone and the initial acetone concentration was the most important parameter in determining energy efficiency of the plasma-catalytic process. Moreover, the interactions between flow rate and initial concentration impose a significant effect on the plasma-catalytic process for acetone removal.

Acknowledgements

This work is financially supported by National Natural Science Foundation of China (No. 51206143), National Science Fund for Distinguished Young Scholars (No. 51125025) and the Royal Society (UK).

References

Aerts, R., Tu, X., Van Gaens, W., Whitehead, J.C., Bogaerts, A., 2013. Gas purification by nonthermal plasma: a case study of ethylene. Environ. Sci. Technol. 47, 6478-6485.

Águila, G., Gracia, F., Cortés, J., Araya, P., 2008. Effect of copper species and the presence of reaction products on the activity of methane oxidation on supported CuO catalysts. Appl. Catal. B: Environ. 77, 325-338.

An, H.T.Q., Huu, T.P., Le Van, T., Cormier, J.M., Khacef, A., 2011. Application of atmospheric non thermal plasma-catalysis hybrid system for air pollution control: Toluene removal. Catal. Today 176, 474-477.

Butron-Garcia, M.I., Jofre-Reche, J.A., Martin-Martinez, J.M., 2015. Use of statistical design of experiments in the optimization of Ar-O_2 low-pressure plasma treatment conditions of polydimethylsiloxane (PDMS) for increasing polarity and adhesion, and inhibiting hydrophobic recovery. Appl. Surf. Sci. 332, 1-11.

Chang, C.L., Lin, T.S., 2005. Decomposition of toluene and acetone in packed dielectric barrier discharge reactors. Plasma Chem. Plasma Proces. 25, 227-243.

Chen, H.L., Lee, H.M., Chen, S.H., Chang, M.B., Yu, S.J., Li, S.N., 2009. Removal of volatile organic compounds by single-stage and two-stage plasma catalysis systems: A review of the performance enhancement mechanisms, current status, and suitable applications. Environ. Sci. Technol. 43, 2216-2227.

Flowers, L., Broder, M.W., Forsyth, C., 2003. Toxicological review of acetone. Environment Protection Agency.

Fridman, A.A., 2008. Plasma chemistry. Cambridge University Press.

Guo, Y.F., Ye, D.Q., Chen, K.F., He, J.C., 2007. Toluene removal by a DBD-type plasma combined with metal oxides catalysts supported by nickel foam. Catal Today 126, 328-337.

Huang, H., Ye, D., Leung, D.Y.C., Feng, F., Guan, X., 2011. Byproducts and pathways of toluene destruction via plasma-catalysis. J. Mol. Catal. A: Chem. 336, 87-93.

Kim, H.-H., 2004. Nonthermal plasma processing for air-pollution control: A historical review, current issues, and future prospects. Plasma Proces. Polym. 1, 91-110.

Kogelschatz, U., 2003. Dielectric-barrier discharges: Their history, discharge physics, and industrial applications. Plasma Chem. Plasma Proces. 23, 1-46.

Koppmann, R., 2008. Volatile organic compounds in the atmosphere. John Wiley & Sons.

López-Suárez, F.E., Bueno-López, A., Illán-Gómez, M.J., 2008. Cu/Al_2O_3 catalysts for soot oxidation: Copper loading effect. Appl. Catal. B: Environ. 84, 651-658.

Lippens, B.C., De Boer, J., 1965. Studies on pore systems in catalysts: V. The t method. Journal of Catalysis 4, 319-323.

Luo, M.F., Fang, P., He, M., Xie, Y.L., 2005. In situ XRD, Raman, and TPR studies of CuO/Al_2O_3 catalysts for CO oxidation. J. Mol. Catal. A: Chem. 239, 243-248.

Lyulyukin, M.N., Besov, A.S., Vorontsov, A.V., 2010. The influence of corona electrodes thickness on the efficiency of plasmachemical oxidation of acetone. Plasma Chem. Plasma Proces. 31, 23-39.

Magne, L., Blin-Simiand, N., Gadonna, K., Jeanney, P., Jorand, F., Pasquiers, S., Postel, C., 2009. OH kinetics in photo-triggered discharges used for VOCs conversion. Eur. Phys. J. Appl. Phys. 47, 22816.

Mei, D., He, Y.L., Liu, S., Yan, J., Tu, X., 2015. Optimization of CO_2 conversion in a cylindrical dielectric barrier discharge reactor using design of experiments. Plasma Proces. Polym.

Montgomery, D.C., Montgomery, D.C., Montgomery, D.C., 1984. Design and analysis of experiments. Wiley New York.

Mousavi, S.M., Salari, D., Niaei, A., Panahi, P.N., Shafiei, S., 2014. A modelling study and optimization of catalytic reduction of NO over CeO_2-MnO_x(0.25)-Ba mixed oxide catalyst using design of experiments. Environ. Technol. 35, 581-589.

Narengerile, Watanabe, T., 2012. Acetone decomposition by water plasmas at atmospheric pressure. Chem. Engin. Sci. 69, 296-303.

Nie, Y., Zheng, Q., Liang, X., Gu, D., Lu, M., Min, M., Ji, J., 2013. Decomposition treatment of SO_2F_2 using packed bed DBD plasma followed by chemical absorption. Environ. Sci. Technol. 47, 7934-7939.

Samukawa, S., Hori, M., Rauf, S., Tachibana, K., Bruggeman, P., Kroesen, G., Whitehead, J.C., Murphy, A.B., Gutsol, A.F., Starikovskaia, S., Kortshagen, U., Boeuf, J.P., Sommerer, T.J., Kushner, M.J., Czarnetzki, U., Mason, N., 2012. The 2012 Plasma Roadmap. Journal of Physics D: Appl. Phys. 45, 253001.

Schnelle Jr, K.B., Brown, C.A., 2001. Air pollution control technology handbook. CRC press.

Sing, K.S., 1985. Reporting physisorption data for gas/solid systems with special reference to the determination of surface area and porosity (Recommendations 1984). Pure Appl. Chem. 57, 603-619.

Thevenet, F., Sivachandiran, L., Guaitella, O., Barakat, C., Rousseau, A., 2014. Plasma-catalyst coupling for volatile organic compound removal and indoor air treatment: a review. J. Phys. D: Appl. Phys. 47, 224011.

Trinh, H.Q., Mok, Y.S., 2014. Plasma-catalytic oxidation of acetone in annular porous monolithic ceramic-supported catalysts. Chem. Eng. J. 251, 199-206.

Tu, X., Whitehead, J.C., 2012. Plasma-catalytic dry reforming of methane in an atmospheric dielectric barrier discharge: Understanding the synergistic effect at low temperature. Appl. Catal. B: Environ. 125, 439-448.

Van Durme, J., Dewulf, J., Leys, C., Van Langenhove, H., 2008. Combining non-thermal plasma with heterogeneous catalysis in waste gas treatment: A review. Appl. Catal. B: Environ. 78, 324-333.

Vandenbroucke, A.M., Morent, R., De Geyter, N., Leys, C., 2011. Non-thermal plasmas for non-catalytic and catalytic VOC abatement. J. Hazard. Mater. 195, 30-54.

Wu, J.L., Huang, Y.X., Xia, Q.B., Li, Z., 2013. Decomposition of toluene in a plasma catalysis system with NiO, MnO_2, CeO_2, Fe_2O_3, and CuO catalysts. Plasma Chem. Plasma Proces. 33, 1073-1082.

Xu, N., Fu, W., He, C., Cao, L., Liu, X., Zhao, J., Pan, H., 2014. Benzene removal using non-thermal plasma with CuO/AC catalyst: Reaction condition optimization and decomposition mechanism. Plasma Chem. Plasma Proces. 2014, 34, 1387-1402.

Yamamoto, T., Tanaka, T., Kuma, R., Suzuki, S., Amano, F., Shimooka, Y., Kohno, Y., Funabiki, T., Yoshida, S., 2002. NO reduction with CO in the presence of O_2 over Al_2O_3-supported and Cu-based catalysts. Phys. Chem. Chem. Phys. 4, 2449-2458.

Zakaria, Z.Y., Linnekoski, J., Amin, N.A.S., 2012. Catalyst screening for conversion of glycerol to light olefins. Chem. Eng. J. 207, 803-813.

Zheng, C., Zhu, X., Gao, X., Liu, L., Chang, Q., Luo, Z., Cen, K., 2014. Experimental study of acetone removal by packed-bed dielectric barrier discharge reactor. J. Ind. Eng. Chem. 20, 2761-2768.

Zhu, X., Gao, X., Qin, R., Zeng, Y., Qu, R., Zheng, C., Tu, X., 2015a. Plasma-catalytic removal of formaldehyde over Cu-Ce catalysts in a dielectric barrier discharge reactor. Appl. Catal. B: Environ. 170-171, 293-300.

Zhu, X., Gao, X., Yu, X., Zheng, C., Tu, X., 2015b. Catalyst screening for acetone removal in a single-stage plasma-catalysis system. Catal. Today, 101-114.